ELSEVIER

Journal of Nuclear Materials 306 (2002) 99–104

journal of nuclear materials

www.elsevier.com/locate/jnucmat

Iodine release from oxidised Zircaloy cladding in contact with an alkaline solution

K. Poulard [a,*], A. Chevarier [a], N. Moncoffre [a], D. Crusset [b]

[a] *Institut de Physique Nucléaire de Lyon, IN2P3-CNRS, 43 Bd du 11 Novembre 1918, F-69622 Villeurbanne cedex, France*
[b] *ANDRA Parc de la Croix Blanche 1-7 rue Jean Monnet, F-92298 Châtenay-Malabry cedex, France*

Received 18 February 2002; accepted 4 July 2002

Abstract

During reactor processing, fission products, among which iodine, are implanted by recoil inside the Zircaloy cladding tube. At the same time, oxidation of the cladding tube occurs, hence in the waste storage phase, zirconia acts as a migration barrier. Before chemical separation, the cladding tubes are sectioned into pieces called hulls in order to release the UO_2 pellets which are rendered soluble in nitric acid. The hulls are collected as a solid waste and were embedded inside a concrete structure until 1995. In the perspective of geological storage, a great interest is given to iodine release processes in order to model and to extrapolate them to large time scales. In order to analyse the mechanisms involved in iodine migration, iodine atoms were introduced in Zircaloy oxidized samples by means of ion implantation. Corrosion tests were performed in order to simulate the impact of infiltrated water in the concrete disposal. Iodine release was measured by Rutherford backscattering spectroscopy. Processes responsible for iodine release are analysed.

PACS: 61.85; 52.77.D; 68.43.V

1. Introduction

In the pressurised water reactors, the cladding tubes made of Zircaloy-4 are oxidised through several micrometers of the internal face by direct contact with the UO_2 pellets [1]. At the same time, fission products are implanted by recoil, most of them being located in the first micrometers of the oxide layer [2,3]. During reprocessing, the cladding tubes are cut up and washed with nitric acid in order to dissolve the spent fuel. Until 1995, the sections of cladding tubes, called hulls, were immobilised in a concrete matrix. From the point of view of geological storage, it is necessary to understand the mechanisms involved in the radioactivity release at the time of the contact between the hulls and the infiltrated water in the concrete structures. In this paper, we will focus on iodine, since it is a volatile fission product and because of ^{129}I, which is a very long half-life isotope ($T = 1.59 \times 10^7$ years). Moreover, it has been demonstrated [4] that most of the iodine ions are distributed in the first 2 μm of the inner cladding tube, their surface concentration being larger than 10^{14} atoms cm^{-2}. For these reasons, it is of primary importance to study phenomena occurring at the very near surface. The experiments were performed on Zircaloy-4 oxidised samples, implanted at the surface. In order to simulate the infiltrated water in the concrete matrix during storage, the samples were put in contact with a basic solution (pH = 13.5 at 25 °C) in a nickel autoclave. The challenge is to model the sample evolution in this solution. It implies the study of the different parameters responsible for the iodine release. Therefore, the iodine evolution was compared to the europium surface marker one. The

* Corresponding author. Tel.: +33-472 431 063/057; fax: +33-472 448 040/004.
E-mail address: poulard@ipnl.in2p3.fr (K. Poulard).

0022-3115/02/$ - see front matter
PII: S0022-3115(02)00918-2

influence of the hydroxyl ion penetration in the sample subsurface was evaluated and correlated to the iodine diffusion

2. Evidence of the iodine release

2.1. Experimental procedure

During reactor operation, oxidation of the cladding tube inner surface occurs in the dry atmosphere, therefore we made experiments on Zircaloy-4 pellets (1.7 wt% Sn, 0.24 wt% Fe, 0.13 wt% Cr) annealed under air. As shown in Fig. 1, in the case of 450 °C annealing temperature, the oxide growth follows first a parabolic law corresponding to the formation of a compact zirconia layer, then after the point of transition, the oxidation process accelerates according to a linear kinetic law [5]. Most of the experiments presented in this paper were performed on Zircaloy-4 pellets annealed under air at 450 °C during 5 h. Such conditions correspond to the formation of 0.8 μm pre-transition oxide layers. However, results concerning experiments [6] performed on post-transition oxide layers will be referred to in the discussion.

Iodine implantation into zirconia was carried out at the 'Institut de Physique Nucléaire' (IPN) of Lyon using the 400 kV implantation facility. Iodine was introduced with an energy of 180 keV which corresponds to an average range of 42 nm. The implantation dose was set equal to 10^{16} atom cm^{-2}. Such a dose is larger than the cladding tube iodine contamination (about 10^{14} atom cm^{-2}) but is of the same order of magnitude as the total fission product implantation dose. It also corresponds to the appropriate concentration required to profile iodine by using Rutherford backscattering spectroscopy (RBS). It can also be added that RBS was chosen rather than another analytical method, such as SIMS, since it is a non-destructive technique which allows a step by step profiling of iodine on the same sample. The modifications of the iodine depth distribution due to the corrosion treatment were investigated by RBS experiments at the 4 MV Van de Graaff accelerator of the IPN of Lyon. At each step of the corrosion tests, the RBS analysis was made using He ions with 3 MeV incident energy.

The corrosion tests were performed in an autoclave. The specimens were exposed to a basic solution at 250, 275 and 300 °C. This solution is representative of the infiltrated water through a concrete medium. It was prepared with sodium hydroxide (2.9 $g l^{-1}$) and potassium hydroxide (16.8 $g l^{-1}$). The resulting pH of this solution at 25 °C was 13.5. The corrosion tests were conducted during 12 weeks with regular sampling every two weeks.

2.2. Results

A typical as-recorded spectrum obtained on an oxidised Zircaloy-4 sample iodine implanted is shown in Fig. 2. The signal arising from the various atoms present in the target as well as the oxidized layer thickness are labelled. Iodine distribution profiles are deduced from energetic distributions of backscattered α-particles using a classical RBS simulation programme. These RBS iodine profiles obtained at 250, 275 and 300 °C as function of the corrosion conditions are presented in Fig. 3. The iodine depth distribution of as-implanted samples exhibits a gaussian shape with a mean depth R_p of 42 nm and a depth straggling ΔR_p of 16 nm in agreement with SRIM computer simulations [7]. At 300 °C a very strong release is observed after a 14 day treatment (Fig. 3(a)). No distortion of the gaussian shape distribution is observed, which means that the iodine release concerns the whole implantation depth. Then the iodine concentration remains stable whatever the treatment time. This residual concentration remains at around 0.3 at.%. At 275 °C (Fig. 3(b)), a step by step iodine release is observed but a 42 day treatment is necessary to reach the 0.3 at.% residual iodine concen-

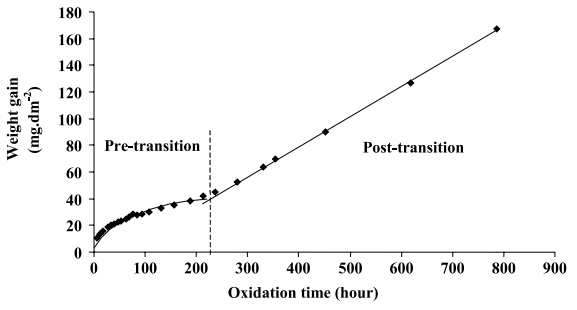

Fig. 1. Weight gain vs. reaction time of Zircaloy-4 samples oxidised in air at 450 °C.

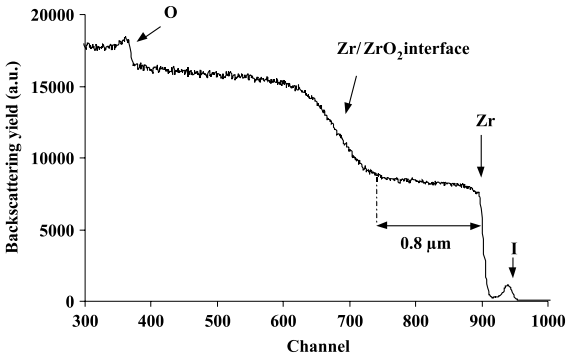

Fig. 2. RBS spectrum recorded on an oxidized Zircaloy sample implanted with iodine ions at a fluence of 10^{16} atom cm^{-2}.

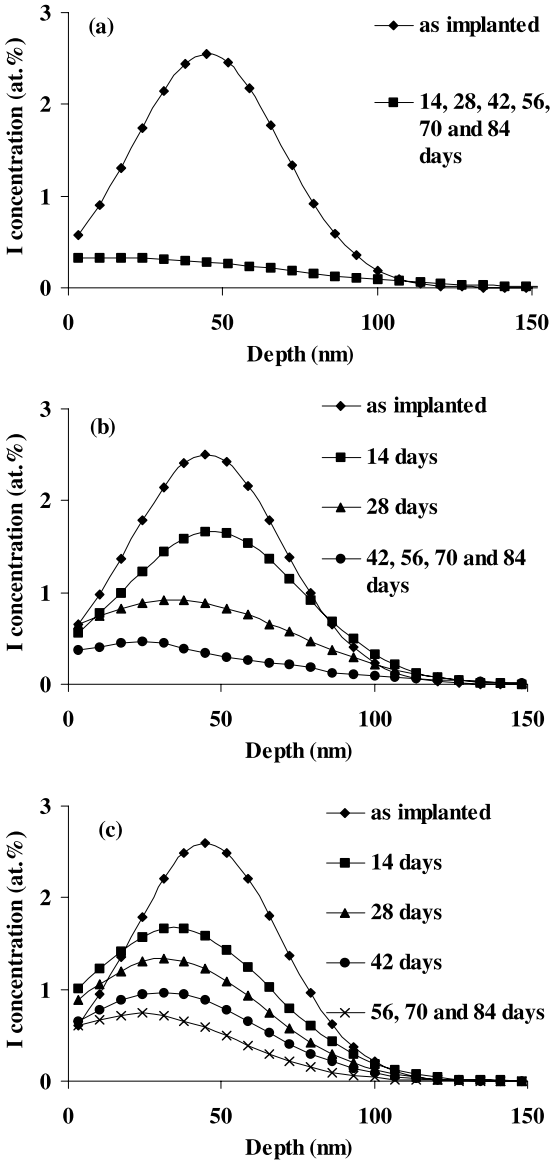

Fig. 3. Iodine profiles as function of the corrosion time at (a) 300 °C, (b) 275 °C and (c) 250 °C.

tration plateau. For the 250 °C treatment (Fig. 3(c)), the rapid release is observed until 56 days. For longer times, 70 and 84 days, iodine concentration in the slow phase remains slightly higher than that at 300 and 275 °C. The integration of the RBS iodine profiles allows the release percentages to be obtained as a function of the treatment time in autoclave. The results are presented in Fig. 4 for the three temperatures. For each temperature one can observe two steps: a rapid release and then a stabilisation of the iodine release. At 275 and 300 °C this stabilisation occurs after a 90% iodine release percentage. The residual dose is then 10^{15} atom cm^{-2}. At 250 °C the

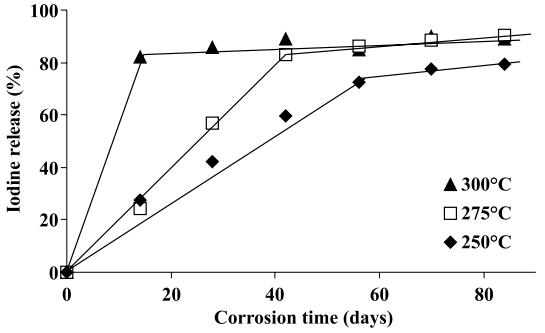

Fig. 4. Iodine release as function of corrosion time at 300, 275 and 250 °C.

stabilisation occurs at 80% corresponding to a remaining dose in the sample of 2×10^{15} iodine cm^{-2}. Complementary, autoclave experiments in pure water (pH = 7 at 25 °C) at 300 °C performed during six weeks on our reference samples lead to iodine releases less then 5%. These results prove that the corrosive medium is responsible for the high rapid iodine release previously observed.

2.3. Influence of the implantation dose on the iodine release.

The slow phase has been observed only for residual doses lower than 10^{15} atom cm^{-2}. In order to study this dose effect, experiments using radioactive ^{131}I were done. Iodine 131 implantations were performed at a dose equal to 10^9 atom cm^{-2}. The autoclave treatments in the basic medium were performed at 300 °C during 4, 8, 12 and 19 days. The iodine release was measured by gamma spectroscopy, the activity of the as-implanted sample being taken as a reference. The iodine release values are given in Table 1. They stand between 3% and 5%, and remain very weak compared to the values observed in the rapid phase for the stable iodine. However, they are of the same order of magnitude as the release percentages (between 3% and 7%) obtained in the slow phase for stable implantations. The experiments seem to confirm that the rapid phase is correlated to a dose effect, and also to the nature of the surrounding medium. In order to assess the latter hypothesis, we measured the

Table 1
Radioactive iodine release as function of treatment time

Autoclave treatment time (days)	^{131}I release (%)
4	2.8
8	3.1
12	4.8
19	5.2

Measurement accuracy is estimated to 0.2%.

zirconia surface corrosion which could be responsible for iodine release in such severe conditions.

3. Study of the zirconia surface corrosion

The partial dissolution [8–10] of the oxide coating was studied using the rare earth element europium as a surface marker of zirconia. Such a choice is based on previous experimental results [11] ensuring that this marker does not diffuse in the 250–300 °C temperature range as its thermal diffusion coefficient is equal to 2×10^{-27} cm^2 s^{-1} at 300 °C. Such a value means that, within 70 days, Eu would migrate over 2×10^{-3} nm. Moreover, an autoclave experiment performed in pure water at 300 °C during six weeks [12] shows that it has no influence on the Eu implanted profiles. It can be thus assumed that Eu diffusivity at 300 °C in an aqueous neutral medium is negligible.

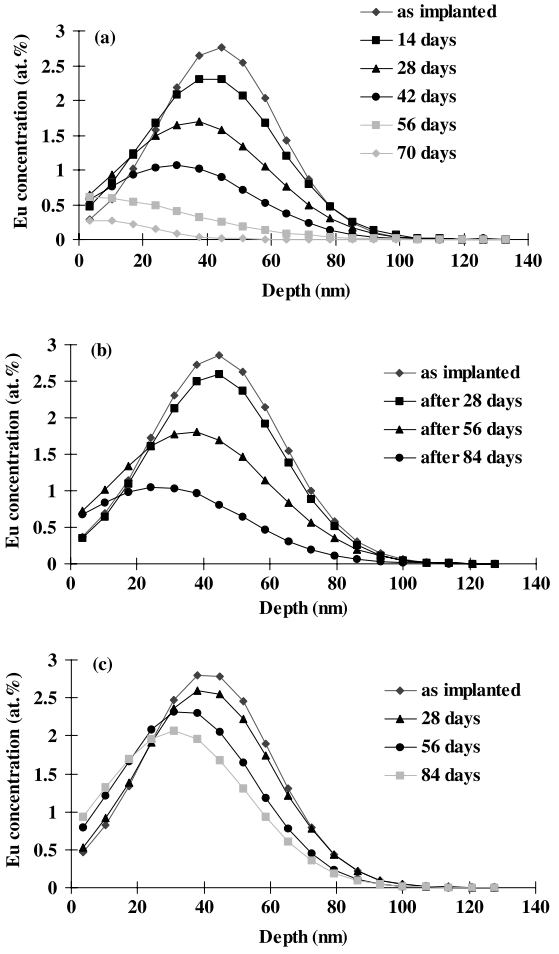

Fig. 5. Europium profile evolution as function of corrosion time in autoclave at (a) 300 °C, (b) 275 °C and (c) 250 °C.

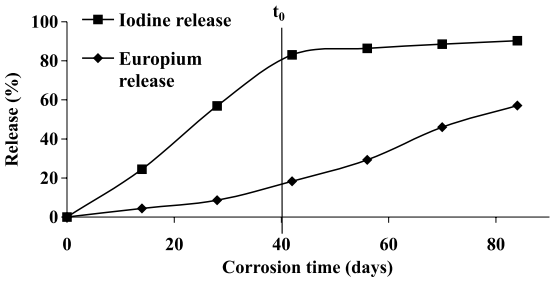

Fig. 6. Comparison between europium and iodine release at 275 °C as function of the corrosion time. The transition time between the rapid phase and the slow phase is noted t_0.

In these experiments, the same procedure in the sample elaboration and in the corrosion tests as the one described in Section 2.1 was followed. The samples were implanted with europium ions instead of iodine ions. According to the SRIM-2000 code, the europium 153 implantation energy was adjusted to 200 keV in order to obtain similar iodine and europium depth distributions. The Eu implantation dose was also set at 10^{16} ions cm^{-2}.

The evolution of the europium concentration profiles measured at each corrosion step are given in Fig. 5 in the 250 and 300 °C temperature range. The spectra evolution, as a function of the corrosion time, is characterised by (i) a decrease in the Eu maximum concentration, (ii) a smooth translation of Eu distributions towards the surface, (iii) a decrease in the Eu global concentrations. From these observations, we deduce that a non-homogeneous dissolution of the zirconia layer occurs in this alkaline medium which was corroborated by scanning electron microscopy surface observations. By integration over the europium depth distributions and taking as a reference the implantation dose, we measured the europium loss percentage. Europium and iodine implantation profiles being identical, the Eu loss is representative of the iodine loss through a zirconia surface dissolution. The results are presented in Fig. 6 and are compared to those of the global iodine release in the 275 °C temperature treatment. In this figure, the time characteristic of the transition between the rapid and the slow phases is noted t_0. This figure shows that the I release is much larger than the Eu one and cannot be explained by the zirconia surface corrosion only. An explanation of this rapid iodine release could be a specific surface chemical interaction of iodine with the basic medium. Let us examine this hypothesis.

4. Evidence of the specific interaction of hydroxyl ions with iodine

In order to evaluate the penetration of the hydroxyl ions in the sample, we performed elastic recoil detection

analysis (ERDA) [13,14] assuming that in such a basic medium the hydrogen profiles will be representative of the OH^- ones. The evolution of the hydrogen concentration in the zirconia matrices was measured as a function of the corrosion time. In order to increase the detection sensitivity of the ERDA technique, we took advantage of the large (^{15}N, H) elastic cross-section at 6.2 MeV. The nitrogen-15 ions scattered on zirconia were stopped in a mylar foil before reaching the detector used to measure the energy distribution of hydrogen recoil atoms.

A comparison between the hydrogen and iodine concentrations integrated over the implanted zone is given in Fig. 7 as a function of the 275 °C autoclave experiment times. After 14, 28 and 42 days, one can observe large iodine releases, while from 56 to 84 days, iodine concentrations at the sample surface remain nearly constant. The hydrogen concentration presents a similar evolution. It decreases strongly between the second (28 days) and the third (42 days) corrosion test and then remains constant. The release of iodine is thus very likely to be connected to the concentration of hydroxyl ions. Nevertheless, we checked that the migration of hydroxyl ions in the zirconia subsurface is not enhanced by defects induced by implantation. For this purpose we measured the hydrogen concentration in zirconia samples implanted with europium ions, chosen for their weak chemical reactivity. As in the corrosion study, europium implantation conditions (200 keV, 10^{16} atom cm^{-2}) were adjusted to the iodine implantation profiles. We then compared the hydrogen profiles of europium and iodine implanted samples and of a non-implanted sample, after a 14 day treatment in autoclave. The results are shown in Fig. 8. One can observe that the hydrogen concentration in non-implanted and in Eu-implanted samples is similar and remains at around 1 at.%. In the case of the iodine implanted sample, the hydrogen content in the implanted depth is larger than 3 at.%. These experiments clearly demonstrate that the hydrogen (representative of hydroxyl) migration in zirconia is enhanced by the presence of iodine in the sample, and that iodine release is correlated to the hydroxyl ion release from the zirconia subsurface.

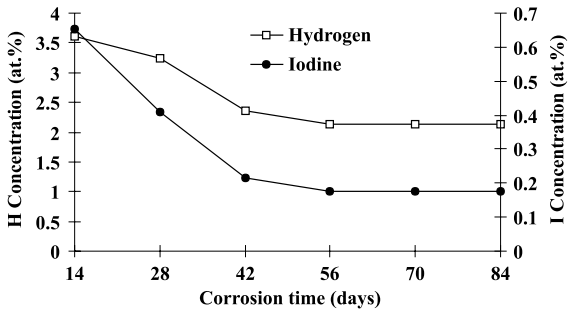

Fig. 7. Comparison between hydrogen and iodine concentrations integrated over the implanted zone as function of the autoclave experiment time.

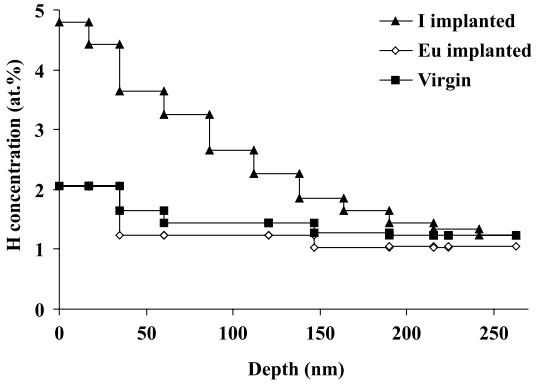

Fig. 8. Comparison of hydrogen concentration profiles observed after a 14 days alkaline treatment at 275 °C on a virgin sample, an Eu implanted sample and an iodine implanted sample.

The correlation between the behaviour of iodine and hydroxyl ions could be explained by the creation of chemical complexes. In the literature [15], we found a possible complexation between iodine, hydroxyl ions and zirconium. This supposes, first the formation of $Zr(OH)_4$ at the solid–liquid interface which can then lead, in the presence of iodine, to the $ZrI(OH)_3$ complex by substitution of an OH^- by an I^-. The oxide layer is degraded by the corrosion in the basic medium thus creating a network of cracks and pores in which $Zr(OH)_4$ can be formed [16]. These complexes can, after their formation, be retained in the disturbed layer of oxide. These phenomena of complexation and retention can explain the observed correlation between the presence of iodine and hydroxyl ions.

5. Conclusion

To conclude, we can show that two phases exist in iodine release from implanted zirconia in contact with a basic medium:

(i) the rapid phase was shown to strongly depend on the implantation dose. The iodine release cannot be explained by a surface dissolution but is correlated with the hydroxyl yield absorbed in the zirconia subsurface,
(ii) the slow phase corresponding to a very small release rate (5%) which has been observed at low iodine concentrations.

We have shown however that a specific correlation between I and OH^- species occur both in the rapid and slow phases. The identification of the mechanism

involved in this coupling would allow to extrapolate our results to geological storage conditions.

References

[1] H. Kleykamp, J. Nucl. Mater. 171 (1990) 181.
[2] T. Hirabayashi, T. Sato, C.N. Sagawa, M. Masaki, M. Saeki, T. Adaci, J. Nucl. Mater. 45 (1990) 174.
[3] R. Restani, E.T. Aerne, G. Bart, H.P. Linder, A. Müller, F. Petrik, Technical Report 92-13, Nagra, Wettingen, Switzerland, 1992.
[4] M. Fregonèse, thesis, Institut National Polytechnique of Grenoble, France, October 1997.
[5] C. Lemaignan, A.T. Motta, Materials Science and Technology – A Comprehensive Treatment, in: R.W. Cahn, P. Haasen, E.J. Kramer (Eds.), Zirconium Alloys in Nuclear Applications, B, 10, 1994, Chapter 7.
[6] K. Poulard, thesis, University of Lyon (IPNL), France, September 2001.
[7] J.F. Ziegler, J.P. Biersack, U. Littmark, The Stopping and Range of Ions in Solids, Pergamon, Oxford, 1985.
[8] H. Corriou, L. Grall, J. Meunier, M. Prelas, H. Willermoz, J. Nucl. Mater. 7 (1962) 320.
[9] Y. Nishini, M. Endo, E. Ibe, T. Yasuba, J. Nucl. Mater. 248 (1997) 292.
[10] B. Cox, C. Wu, J. Nucl. Mater. 224 (1995) 169.
[11] K. Poulard, A. Chevarier, J.C. Duclot, N. Moncoffre, D. Crusset, Nucl. Instrum. and Meth. 161 (2000) 668.
[12] K. Poulard, A. Chevarier, N. Moncoffre, D. Crusset, Nucl. Instrum. and Meth. 181 (2001) 640.
[13] J. L'Ecuyer, C. Brassard, J. Appl. Phys. 47 (1976) 881.
[14] F. Paszti, E. Szilagyi, Nucl. Instrum. and Meth. 54 (1994) 507.
[15] P. Pascal, Nouveau traité de chimie minérale, Masson, Tome, IX, 1963.
[16] B. Fourest, T. Vincent, G. Lagarde, S. Hubert, P. Baudoin, J. Nucl. Mater. 282 (2000) 180.